



Evaluation of the dependence of methyl orange organic pollutant removal rate on the amount of titanium dioxide nanoparticles in MWCNTs-TiO₂ photocatalyst using statistical methods and Duncan's multiple range test

Sedigheh Abbasi^a, Davoud Dastan^b, Ştefan Țălu^c, M. B. Tahir^d, Md. Elias^e, Lin Tao^f and Zhi Li^g

^aCentral Research Laboratory, Esfaryen University of Technology, Esfaryen, Iran; ^bDepartment of Materials Science and Engineering, Cornell University, Ithaca, NY, 14850, USA; ^cThe Directorate of Research, Development and Innovation Management (DMCDI), Technical University of Cluj-Napoca, Cluj-Napoca, Romania; ^dDepartment of Physics, Khwaja Fareed University of Engineering and Information Technology Rahim yar Khan, Pakistan; ^eDepartment of Chemistry, Jagannath University, Dhaka, Bangladesh; ^fSchool of Chemical Engineering, University of Science and Technology Liaoning, Anshan, Liaoning, China; ^gSchool of Materials and Metallurgy, University of Science and Technology Liaoning, Anshan

ABSTRACT

Here, we prepared two kinds of nanocomposites (MCT#1 and MCT#2) involving MWCNTs and TiO₂ nanoparticles. The characterisation of the samples is carried out based on FTIR spectroscopy and TEM. The Ti-O groups that is attributed to the TiO₂ nanoparticles can be confirmed according to the FTIR analysis. TEM images show that the average particle size of TiO₂ nanoparticles in prepare MCT#1 and MCT#2 is equal to 13 nm and 15 nm, respectively. The influences of nanocomposites weight fraction and illumination time are investigated on the decomposition rate of methyl orange (MO) as pollutant. The photocatalytic results exhibit that the decomposition rate of MO is increased with respect to the weight fraction and illumination time. Meanwhile, higher decomposition rate can be observed using MCT#2 compared to MCT#1. Statistical analysis of the results based on Duncan's multiple range test at $\alpha = 0.05$ reveals that all of the applied levels of the factors have a significant effect on the decomposition rate. The response surface results confirm that the effect of illumination time is high that that of weight fraction of MCT#1 and MCT#2.

ARTICLE HISTORY

Received 12 January 2022
Accepted 15 March 2022

KEYWORDS

MWCNTs; TiO₂ nanoparticles; decomposition rate; statistical analysis; duncan's test; response surface

1. Introduction

Organic dyes are commonly applied in different industries such as textile and dyestuff. Some of these organic dyes, which are often toxic, can be entered in the sewage of the industries that is discharged into water systems. It can be leads to the significant environmental pollutions [1]. Coloured pollutants reduce the amount of sunlight penetrating deep into the water and disrupt the photosynthetic process of aquatic organisms [2,3]. Therefore, reducing or eliminating dye

contaminants from industrial wastewater is critical to protecting the environment. In recent years, various methods including reverse osmosis, ozonisation, photocatalytic degradation and adsorption have been studied for the decomposition of dye contaminants [4,5]. Among the mentioned techniques, advanced oxidation process (AOP) using semiconductor photocatalysts is an efficient technique that can completely decompose the dye organic pollutants [6,7]. TiO_2 due to the wide band gap (3.2 eV) is applied as a dominant photocatalyst for the photocatalytic oxidation of environmental organic pollutants. The AOP is based on the irradiation of suspension containing the pollutant and semiconductor using UV light source. The UV irradiation leads to the excitation of electrons that are located in the valence band of the semiconductors. The excited electrons can transmit from the valence band to the conduction band [8,9]. Therefore, due to the migration of an electron from the valence layer to the conduction layer, a hole and an electron are produced on the valence band and conduction band, respectively. The generated electron and hole pairs have a significant effect on the degradation of pollutants [10,11]. The recombination of the produced charges can reduce the degradation rate of pollutants. Therefore, it leads to the enhancement of operating cost and decreasing the removal efficiency. The coupling of TiO_2 nanoparticles with materials that have a high aspect ratio is expected to preparation of a novel nanocomposite, which can reduce the recombination rate of generated electron and hole pairs [12]. In the recent years, there are several reports that studied the effect of different supports such as carbon nanotubes (CNTs), graphene oxide (GO) and reduced graphene oxide (rGO) on the recombination rate of produced electron and hole pairs [13–15]. The reported results show that the coupled systems containing applied support and semiconductor have higher photocatalytic performance rather than the semiconductor alone. It can be related to the positive influence of support on the decrement on recombination rate [16,17]. Multi-walled carbon nanotubes (MWCNTs) are widely applied for preparation of nanocomposites, sensors and nanoelectronics [18,19]. It can be due to the excellent physical, mechanical, electrical, thermal and chemical properties of MWCNTs [20]. Recently, the application of MWCNTs for synthesis of catalytic template materials has great deal of attention due to the unique high surface area and excellent aspect ratio. Meanwhile, the coupled MWCNTs@ TiO_2 have been applied as photocatalyst for degradation of different kinds of organic pollutants such as methyl orange (MO) and methylene blue (MB). However, the effect of TiO_2 content in the prepared coupled system has not yet been investigated. In addition, there is no report on the statistical analysis of the photocatalytic performance of MWCNTs@ TiO_2 .

In this study, we prepare a new nanocomposite containing MWCNTs and TiO_2 nanoparticles. The synthesised samples are characterised using Fourier transform infrared (FTIR) and transmission electron microscopy (TEM). The photocatalytic performance of the synthesised samples is evaluated based on the decomposition of MO as organic dye pollutant model. The statistical analysis of the photocatalytic results are carried out based on Duncan's multiple range test and response surface method (RSM).

2. Experimental

2.1. Preparation of MCT nanocomposites

The applied multi-walled carbon nanotube (MWCNTs) in this study have the average diameter around 40–60 nm and length 5–15 μm . The typical method for preparation of the oxidised MWCNTs is based on the acid-treatment of pristine MWCNTs in HNO_3 that is described in our previous works [18,21]. The prepared oxidised MWCNTs contain the functional groups that can be applied for synthesised the TiO_2 @MWCNTs composites. For this purpose, 0.08 g of oxidised MWCNTs is dispersed in 100 ml of distilled water and processed in ultrasonic bath for about 30 min. Subsequently, the desired amount of tetra chloride titanium (TiCl_4 , 99%, Merck) is added to the oxidised MWCNTs suspension as precursor of TiO_2 nanoparticles. The obtained mixture is agitated at ambient temperature for about 5 h. Then the temperature is increased until 65°C for about 12 h. Finally, the suspension is filtered, washed and calcined at 350°C for 3 h. It should be mentioned that by variation of TiCl_4 content, we can synthesis different kinds of nanocomposites. Therefore, in this study, the TiCl_4 content is varied from 0.4 ml to 0.8 ml and the synthesised samples are indexed as MCT#1 and MCT#2, respectively.

2.2. Characterisation

The surface functional groups of the prepared nanocomposites are determined using a Tensor 70 Fourier transform infrared (FTIR) spectrometer. The morphology, decoration quality and particle size of TiO_2 nanoparticles are determined by transmission electron microscopy (TEM, LEO 912AB). The decomposition rate of MO as an organic dye pollutant model is evaluated using UV-Vis absorption spectroscopy (Lambda EZ 201 spectrophotometer, Perkin Elmer Company). For evaluation of the MO decomposition, the specific amount of MCT#1 and MCT#2 (0.1, 0.2 and 0.3%wt) as photocatalyst is added to 80 mL of MO solution (10 ppm). The prepared suspensions are stirred for 60 min in a dark chamber. It leads to the adsorption and desorption equilibrium. The absorbance of the MO in the suspension is recorded at 464 nm. The recorded absorbance is assigned as initial absorbance (A_0) that can be attributed to the initial concentration (C_0). Then, the suspension is irradiated using an Hg vapour lamp (150 W). The absorbance of the MO at each 5 min interval is evaluated and assigned as A_t , which is corresponded to the remained concentration (C_t). The decomposition rate of MO can be calculated based on the Equation 1 [4,14].

$$(\text{Decompositionrate})^{-1} = \frac{C_t}{C_0} \quad (1)$$

3. Results and discussion

3.1. FTIR analysis

Figures 1 and 2 illustrate the Fourier transform infrared (FTIR) spectrums of MCT#1 and MCT#2, respectively. As can be observed in Figure 1, two detectable transmission bands around 1625 cm^{-1} and 3419 cm^{-1} are assigned to the stretching vibration of O-H [18] bonds that is present in the generated carboxylic groups ($\text{HO-C}=\text{O}$) during the oxidation

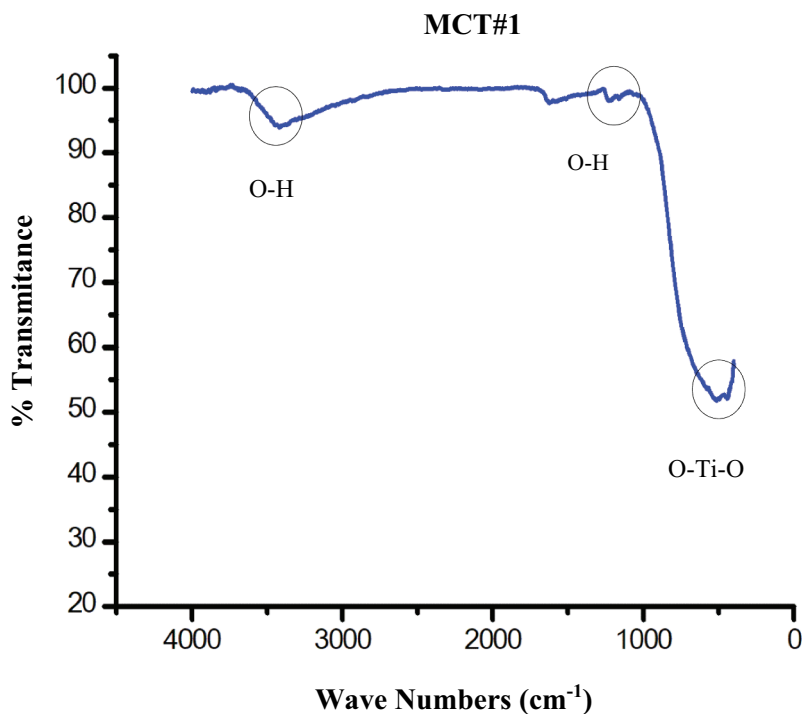


Figure 1. FTIR spectra of MCT#1.

of MWCNTs in NH_3 . The presence of these kinds of oxygen containing groups on the surface of MWCNTs can enhance the hydrophilic properties. Therefore, the stability of MWCNTs in the organic solutions is improved. Meanwhile, these functional groups can act as active sites for nucleation of different kinds of nanoparticles. Besides these two bands, there is a major peak in the range of 440 cm^{-1} to 520 cm^{-1} that can be attributed to the O-Ti bending of TiO_2 nanoparticles [18,22]. The results of Figure 2 reveal that all of the three mentioned transmission bands that are observed in MCT#1 can be detected for synthesised MCT#2. Therefore, it can be confirmed that the hydrolysis of TiCl_4 in the solution containing functionalised MWCNTs can lead to the synthesis of TiO_2 nanoparticles and covalent attachment on the sidewalls of MWCNTs. The comparison between the intensity of Ti-O groups in MCT#1 and MCT#2 reveals that the content of TiO_2 nanoparticles in the prepared MCT#2 is higher than that of MCT#1. It can be attributed to the applied amount of TiCl_4 as precursor of TiO_2 nanoparticles in the hydrolysis process.

3.2. TEM study

Figures 3 and 4 show the TEM images of the synthesised MCT#1 and MCT#2, respectively. According to these figures, the presence of TiO_2 nanostructures with a spherical shape can be confirmed on the outer surface of MWCNTs. Comparison between TEM images of MCT#1 and MCT#2 confirms that the amount of introduced TiO_2

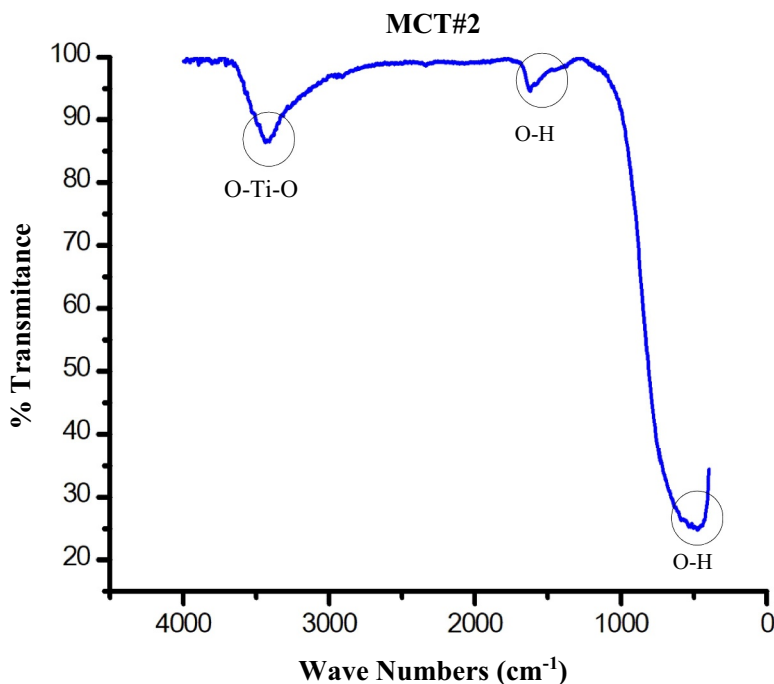


Figure 2. FTIR spectra of MCT#2.

nanostructures on the sidewalls of MCT#1 is lower than that of MCT#2. It can be due to the amount of soluble Ti^{+4} ions in the suspension of MWCNTs. As the amount of applied TiCl_4 as precursor of TiO_2 nanostructures in the synthesis of MCT#2 is higher than that of MCT#1, the produced soluble ions can be enhanced due to the hydrolysis. Therefore, most of ions bind to the negative charges on the surface of MWCNTs ($-\text{COOH}$ and $-\text{OH}$) and cause nucleation [23]. The particle size distributions of decorated TiO_2 nanoparticles on the sidewalls of MCT#1 and MCT#2 are represented if Figures 5 and 6, respectively. The particle size distributions reveal that the particle size of TiO_2 nanostructures in the synthesised MCT#1 and MCT#2 are ranging from 5 nm to 25 nm and 10 nm to 20 nm, respectively. However, the average particle size of the most decorated nanoparticles in the synthesised MCT#1 and MCT#2 are about 13 nm and 15 nm, respectively.

3.3. Degradation rate study

Figures 7 and 8 show the variation of the ratio of MO concentration at each interval to the initial concentration with respect to the irradiation time and weight fraction of the synthesised MCT#1 and MCT#2, respectively. According to these Figures, it is clear that the ratio of MO concentration at each irradiation time to the initial concentration decreases by enhancement of time and weight fraction. It means that the enhancement of time and weight fraction of applied catalysts leads to the decreasing of organic pollutant

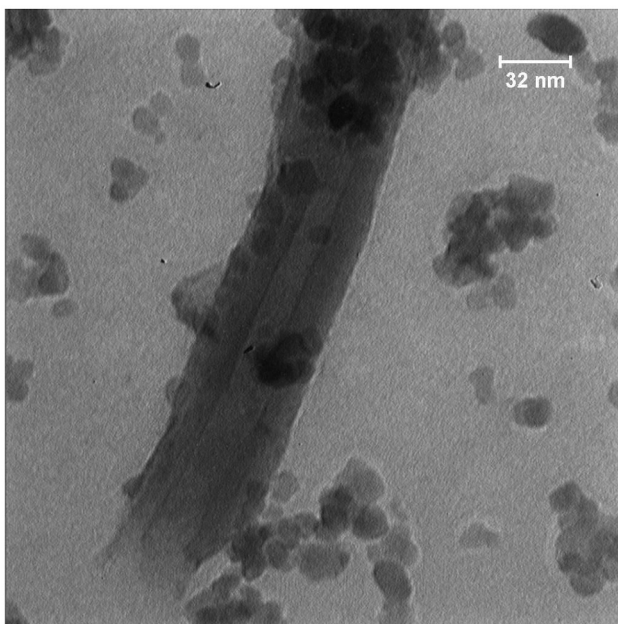


Figure 3. TEM image of MCT#1.

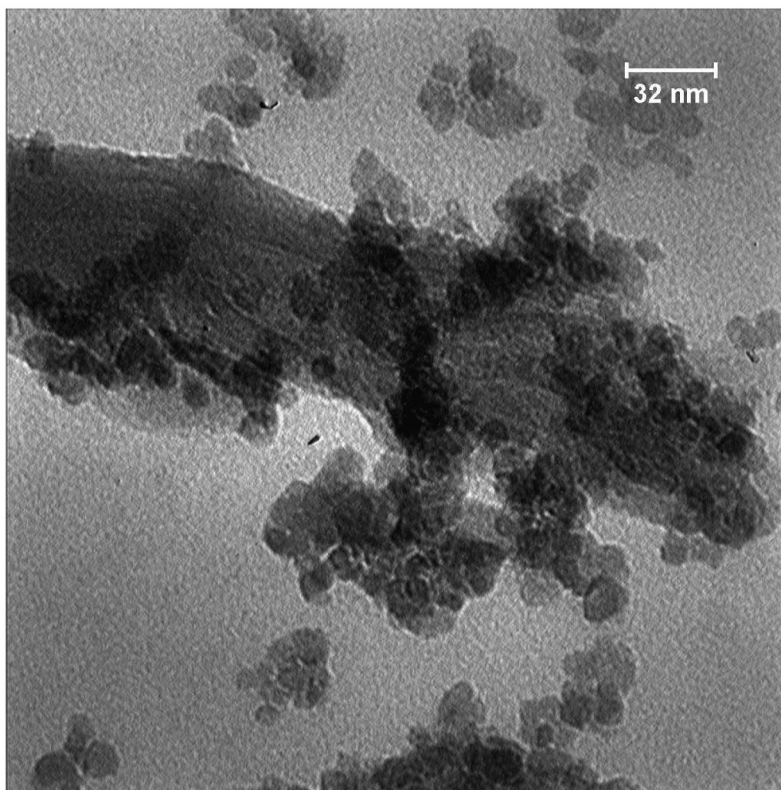


Figure 4. TEM image of MCT#2.

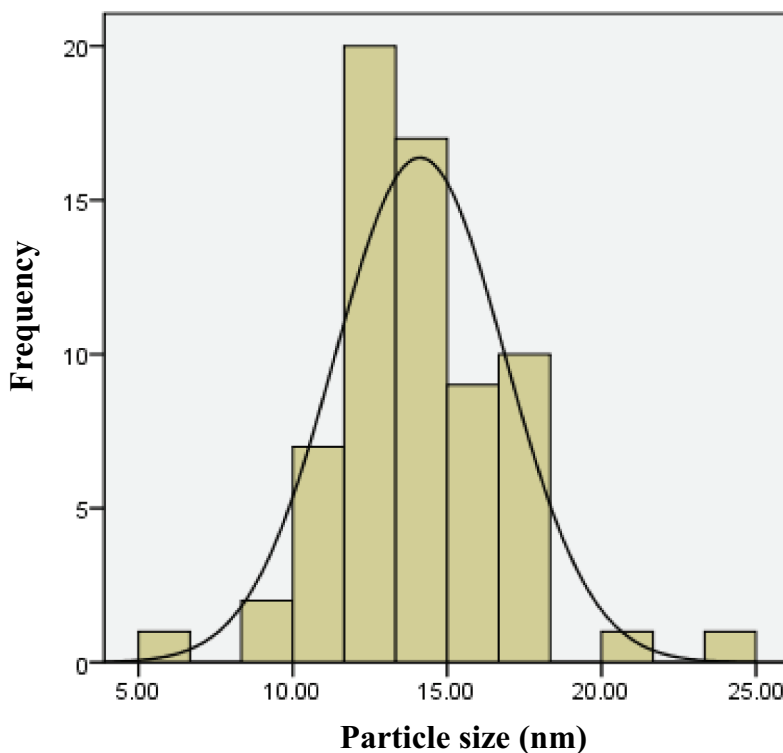


Figure 5. Particle size distribution of coated TiO₂ nanoparticles on the surface of MCT#1.

concentration. The influence of irradiation time on the decomposition of organic pollutants can be due to the excited and transmitted electrons from valence band to the conduction band [24–26]. In fact, UV-irradiation of the photocatalysts surface stimulates the capacitance layer electrons. Thus, the excited electrons transfer to the conduction layer. The transfer of electron from the valence band to the conduction band leads to the creation of cavity (h^+) and electron (e^-) in the conduction band and valence band, respectively. The number of created $e^- - h^+$ pairs is equal to the number of transferred electrons. Thus, as the UV irradiation time increases, the number of transferred electrons and consequently the number of created $e^- - h^+$ pairs increases. The created $e^- - h^+$ pairs can react with the dissolved oxygen in the suspension to form the active oxidising radicals such as hydroxyl (OH \cdot). Therefore, the number of formed oxidising radicals can be enhanced with increasing the irradiation time [6,24]. The reduction of MO concentration with enhancement of the applied photocatalysts concentration (MCT#1 and MCT#2) is due to the augmentation of the contact surface of the photocatalysts with UV irradiation and organic pollutants. The enhancement of the contact surface leads to the increasing of the excited electrons and the created $e^- - h^+$ pairs [8,10,13]. Therefore, the enhancement of the photocatalysts weight fraction has a positive effect on the decomposition rate of MO.

Figure 9 shows the comparison between variation rates of MO concentration with respect to the irradiation time using synthesised MCT#1 and MCT#2 at different weight fraction. It can be observed that at three studied weigh fractions (0.1%wt, 0.2%wt and 0.3%wt) the

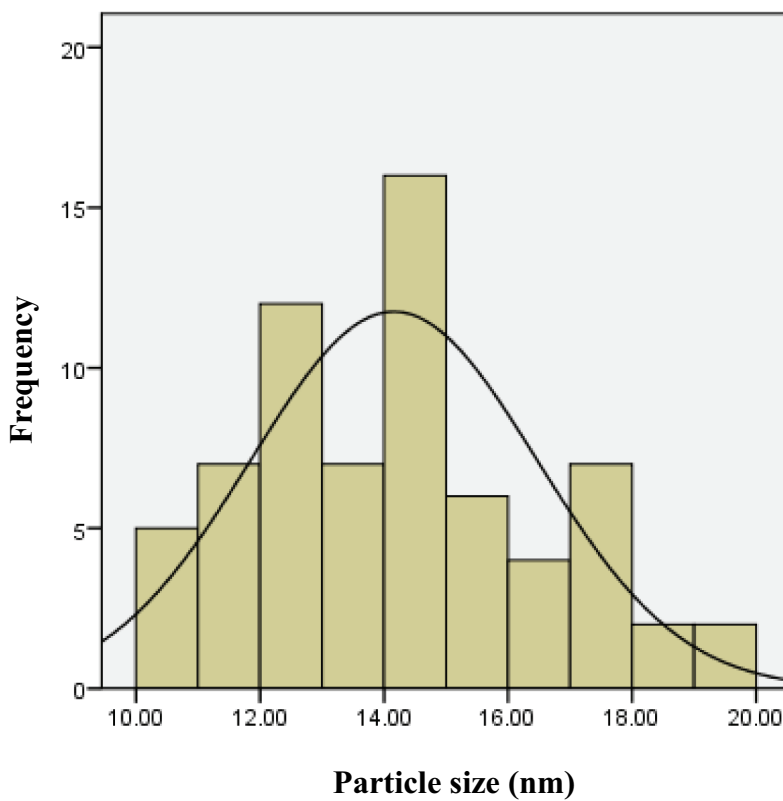


Figure 6. Particle size distribution of coated TiO₂ nanoparticles on the surface of MCT#2.

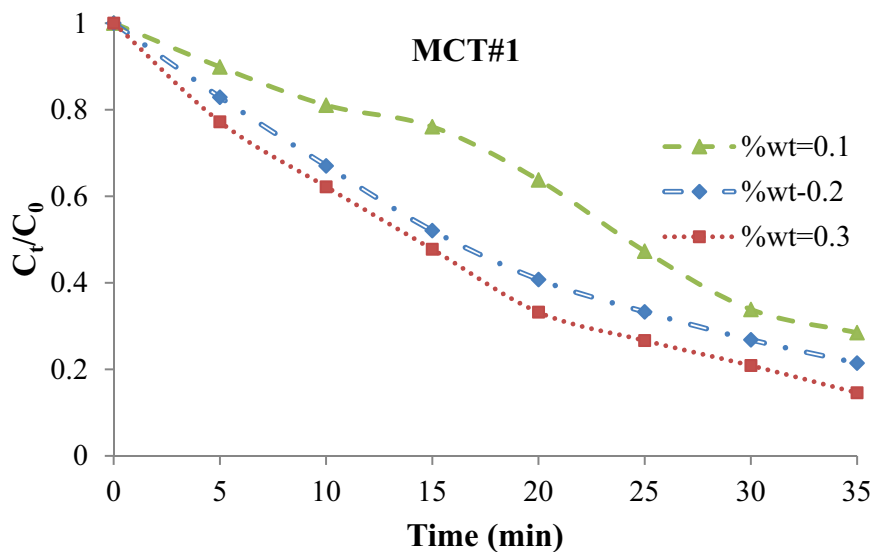


Figure 7. The variation of the ratio of MO concentration at each interval to the initial concentration with respect to the irradiation time and weight fraction of the synthesised MCT#1.

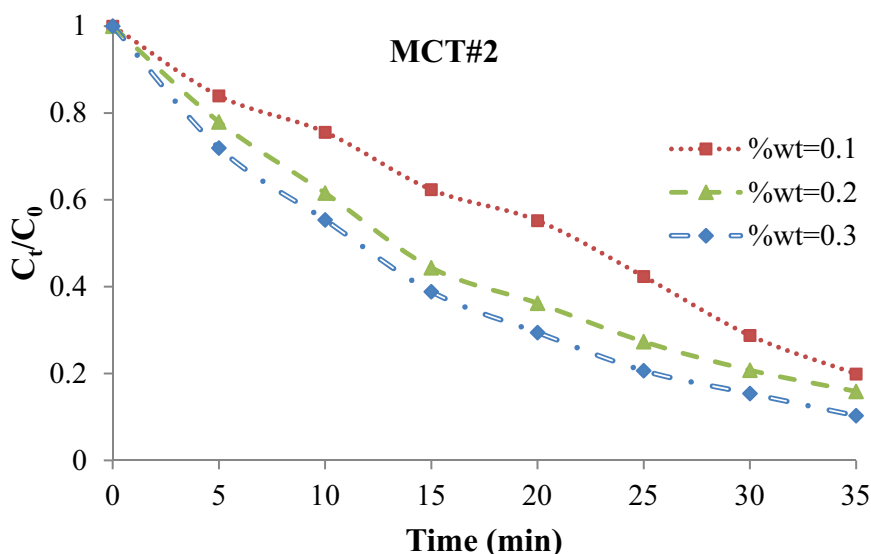


Figure 8. The variation of the ratio of MO concentration at each interval to the initial concentration with respect to the irradiation time and weight fraction of the synthesised MCT#1.

decreasing rate of MO concentration using MCT#2 is higher than that of MCT#1. Therefore, at the same irradiation time the final concentration of MO in the suspension containing MCT#2 is lower than that of MCT#1. It may be due to the amount of decorated TiO₂ nanoparticles on the sidewalls of MWCNTs. Increasing the TiO₂ nanoparticles content leads to the enhancement of active contact surface of photocatalyst that is exposed with UV irradiation. Therefore, it increases the excitation of electrons in the valence band. As the excited electrons are able to move to the conduction layer, the amount of produced e⁻ - h⁺ pairs and active oxidant radicals such as hydroxyl can be increased [14,27,28]. Thus, it can be confirmed that the created oxidising radicals in the suspension containing MCT#2 is greater than MCT#1.

3.4. The statistical analysis based on Duncan's multiple range test

Figures 10 and 11 show the analysis results of MO concentration based on Duncan's multiple range test. The influence of different levels of each main factor such as irradiation time and weight fraction of prepared photocatalysts on the MO concentration can be evaluated according to the Duncan's multiple range test. Figure 10 represents the effect of irradiation time on the variation of MO concentration. According to the Figure 10, it can be observed that the MO concentration decreases by increasing the irradiation time from 5 min to 35 min. It may be due to the effect of irradiation time on the amount of generated electrons and holes [6,25]. Meanwhile, the results of Figure 10 depict that at each irradiation time the MO concentration in the suspension containing synthesised MCT#2 is lower than that of MCT#1. It can be attributed to the TiO₂ content in the synthesised MCT#1 and MCT#2. As mentioned in the before section, the amount of TiO₂ nanoparticles as main photocatalyst in the sample of MCT#2 is higher than that of MCT#1. Therefore, active surface of MCT#2 that is exposure with light source is higher than that of MCT#1. Thus, the excited electrons from valence band to the conduction

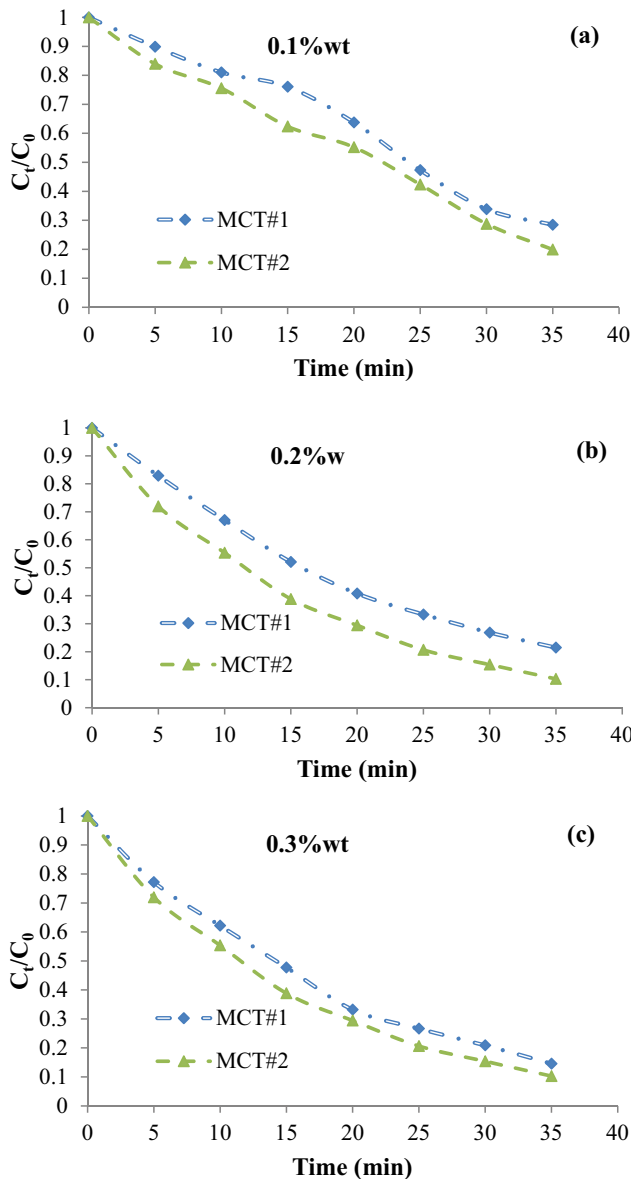


Figure 9. Comparison between variation of the ratio of MO concentration at each interval to the initial concentration with respect to the irradiation time using synthesised MCT#1 and MCT#2 at different weight fraction, a) 0.1%wt, b) 0.2%wt, c) 0.3%wt.

band and formed oxidising radicals can be increased in the suspension involving MCT#2. In addition, the results of Figure 10 confirm that all studied levels of irradiation time have a significant effect on the variation of MO concentration at significance level equal to 0.05.

The influence of weight fractions of MCT#1 and MCT#2 on the variation of MO concentration can be observed in Figure 11. As can be seen, different levels of the weight fractions of prepared MCT #1 and MCT #2 (0.1, 0.2 and 0.3%wt) are significant (at 5% level

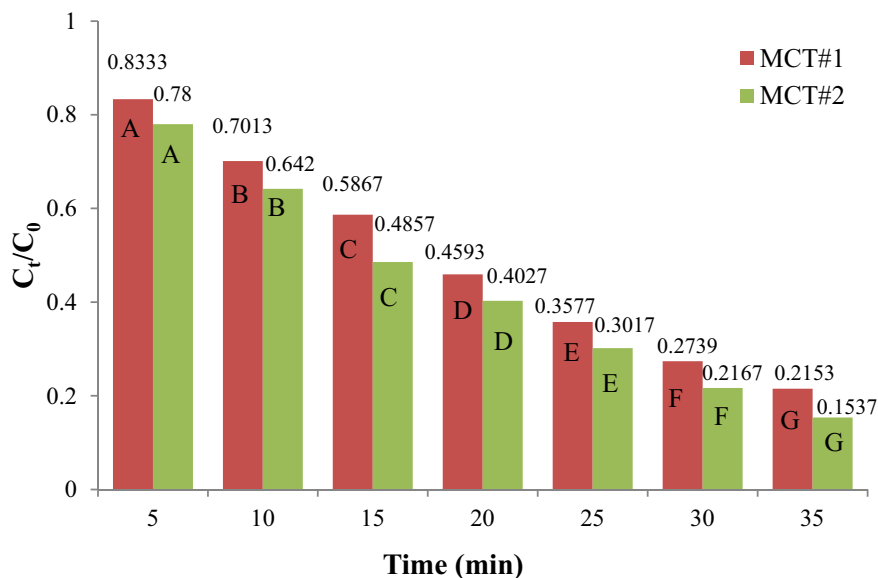


Figure 10. The effect of irradiation time on the MO concentration using synthesised MCT#1 and MCT#2, the analysis based on Duncan's multiple range test at $\alpha = 0.05$.

of probability) on the variation of MO concentration. Meanwhile, it is clear that the degradation rate of MO enhances by increasing the weight fraction of the synthesised MCT #1 and MCT #2. The active surface area of the prepared photocatalysts can be enhanced by increasing the weight fraction of them [9,17]. Therefore, more electrons

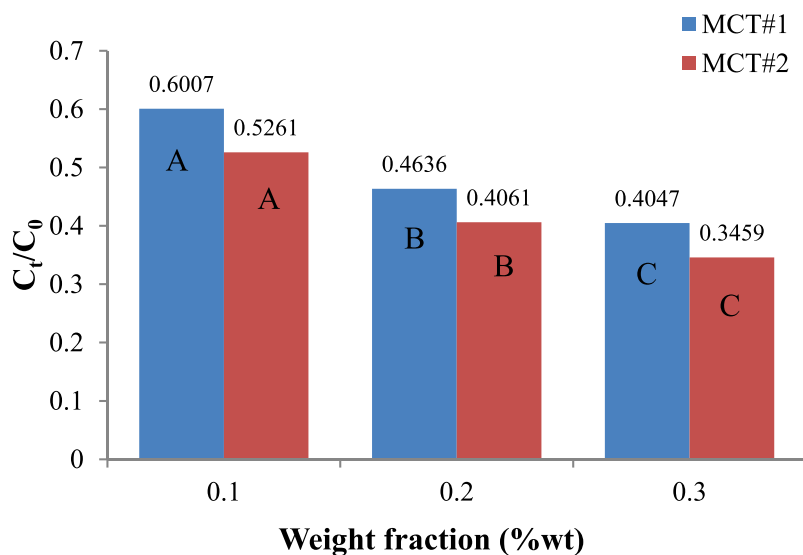


Figure 11. The effect of weight fraction of synthesised MCT#1 and MCT#2 on the MO concentration, the analysis based on Duncan's multiple range test at $\alpha = 0.05$.

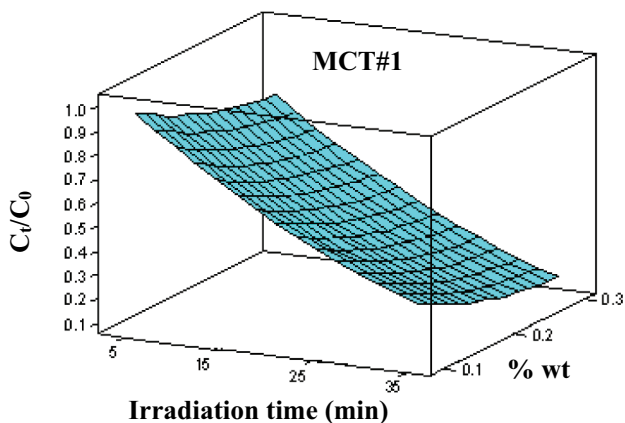


Figure 12. Response surface of the variation of MO concentration using synthesised MCT#1.

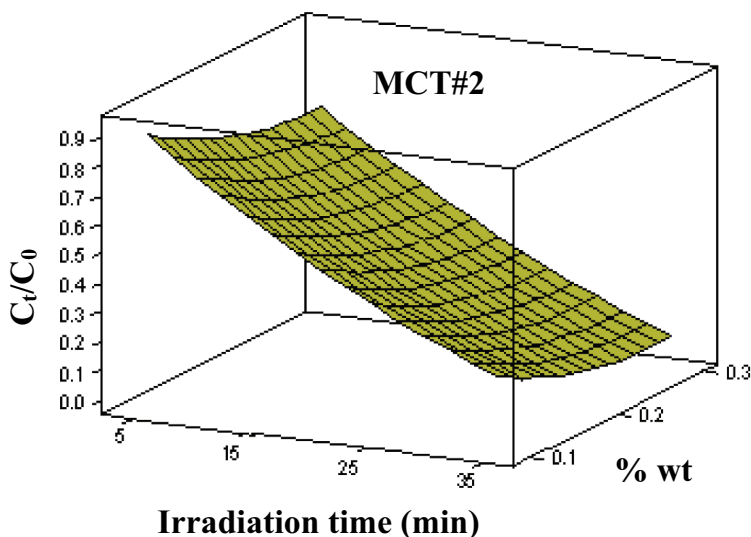


Figure 13. Response surface of the variation of MO concentration using synthesised MCT#2.

can migrate from the valence band to the conduction band. It can be eventuate to the enhancement of the produced active radicals such as hydroxyl (OH.) [14,28] . These kinds of radical can act as decomposer of different dye organic pollutants such as MO.

3.5. Response surface study

Figures 12 and 13 illustrate the response surface of changes in the MO concentration using synthesised MCT#1 and MCT#2, respectively. The response surface method (RSM) is a common graphical approach for investigation the simultaneous influence of the studied parameters (such as irradiation time and weight fraction) on the variation of response (MO concentration). The results of the Figures 12 and 13 confirm that the MO

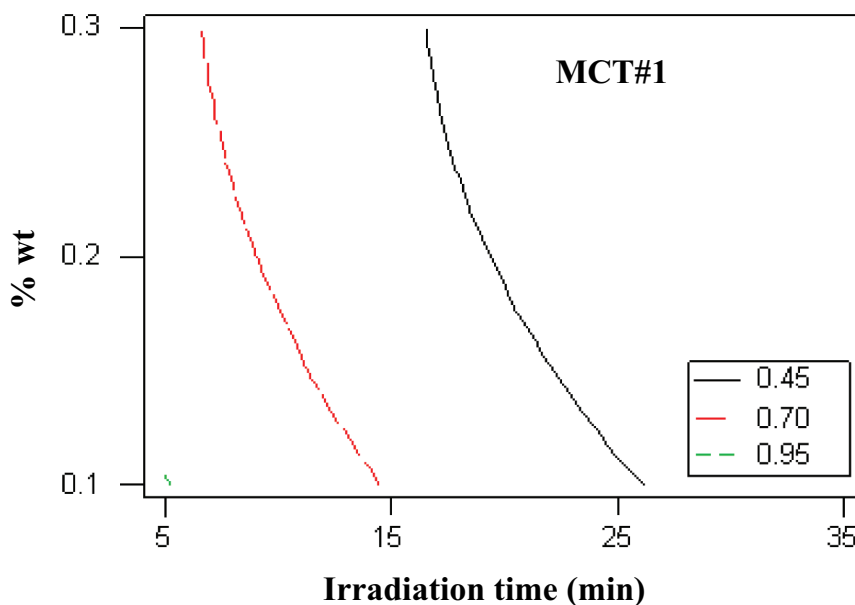


Figure 14. Contour lines of the variation of MO concentration using synthesised MCT#1.

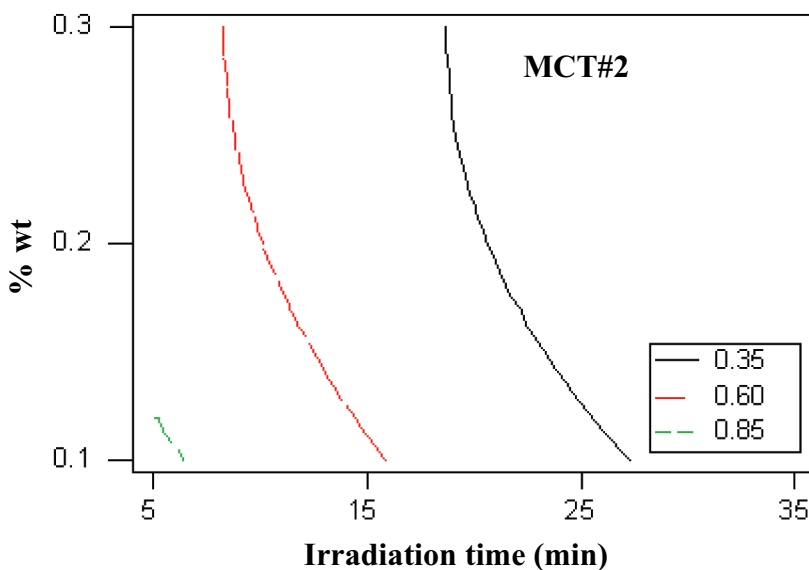


Figure 15. Contour lines of the variation of MO concentration using synthesised MCT#2.

concentration in the presence of synthesised MCT#1 and MCT#2 as photocatalysts decreases by increasing the irradiation time and weight fraction. Although, it can be observed that the influence of irradiation time on the decomposition of MO is more than that of weight fraction. It can be attributed to the effect of irradiation time on the excitation of electrons that are located in the valence band. Thus, the excited electrons

can be transferred from the valence band to the conduction band. It can be eventuated to the formation of electrons and holes in the valence band and conduction band, respectively [2,4]. The produced charges can act as a decomposer of the organic pollutants such as MO. Therefore, the enhancement of generated charges can decrease the MO concentration in the suspension.

Figures 14 and 15 illustrate the contour lines of the variation of MO concentration with respect to the irradiation time and weight fraction of synthesised MCT#1 and MCT#2, respectively. It is clear that the enhancement of irradiation time leads to the decreasing of desired weight fraction of MCT#1 and MCT#2 as photocatalysts. It means that for decreasing the MO concentration to the desired value, the required weight fraction of the both photocatalysts decreases by enhancement of irradiation time.

4. Conclusions

MWCNTs act as substrates for synthesis of TiO₂ nanoparticles via hydrolysis method. TEM images show that TiO₂ nanoparticles are successfully attached on the surface of MWCNTs in the both of MCT#1 and MCT#2. FTIR analysis and TEM images confirm that the TiO₂ nanoparticles content in MCT#2 is higher than that of MCT#1. The photocatalytic results show that the concentration of MO as pollutant is dramatically decreased by enhancement of irradiation time and weight fraction of MCT#1 and MCT#2. Meanwhile, the results confirmed that the photocatalytic performance of MCT#2 is higher than that of MCT#1. The analysis of the results based on response surface depicts that the influence of irradiation time on the degradation of MO is more than that of weight fraction of MCT#1 and MCT#2.

Acknowledgments

The authors of this study appreciated the assistance and cooperation on the central research laboratory of Esfarayen University of Technology.

Disclosure statement

No potential conflict of interest was reported by the author(s).

ORCID

Ştefan Țălu  <http://orcid.org/0000-0003-1311-7657>

Zhi Li  <http://orcid.org/0000-0001-6381-5037>

References

- [1] R. Atchudan, T. Nesakumar Jebakumar Immanuel Edison, S. Perumal et al., *J Photochem Photobiol A Chem* **350**, 75 (2018). doi:10.1016/j.jphotochem.2017.09.038.
- [2] S. Abbasi, *Environ. Monit. Assess.* **191**, 206 (2019). doi:10.1007/s10661-019-7352-0.
- [3] S. Phil Kim, M. Yong Choi and H. Chul Choi, *Appl. Surf. Sci.* **357**, 302 (2015). doi:10.1016/j.apsusc.2015.09.044.
- [4] S. Abbasi, *J Inorg Organomet Polym Mater* **30** (6), 2019.

- [5] M. Ahmad, Z.L.H. E.Ahmed et al., *Ultrason Sonochem* **21** (2), 761 (2014). doi:10.1016/j.ultsonch.2013.08.014.
- [6] S. Abbasi, M. Hasanpour, F. Ahmadpoor et al., *Int J Environ Anal Chem.* **101** (2), 208–224 (2019).
- [7] S. Abbasi, M. Hasanpour and M. Saddat Ekrami Kakhki, *J Mater Sci* **28** (13), 9900 (2017). doi:10.1007/s10854-017-6745-5.
- [8] S. Abbasi, M.-S. Ekrami-Kakhki and M. Tahari, *J Mater Sci* **28** (20), 15306 (2017).
- [9] A. Ghaderi, S. Abbasi and F. Farahbod, *Mater. Res. Express* **5**, 065908 (2018). doi:10.1088/2053-1591/aacd40.
- [10] S. Abbasi and M. Hasanpour, *J Mater Sci* **28** (2), 1307 (2017).
- [11] S. Abbasi and M. Hasanpour, *J Mater Sci* **28** (16), 11846 (2017). doi:10.1007/s10854-017-6992-5.
- [12] R. Atchudan, T. Nesakumar Jebakumar Immanuel Edison, S. Perumal et al. *J Alloys Compd.* **766** (12), 12 (2018); Raji Atchudan, Thomas Nesakumar Jebakumar Immanuel Edison, Suguna Perumal et al., *Journal of Photochemistry and Photobiology A: Chemistry* **333**, 92 (2017). doi:10.1016/j.jallcom.2018.06.272.
- [13] D.A. Reddy, R. Ma and T.K. Kim, *Ceramics Int* **41**, 6999 (2015). doi:10.1016/j.ceramint.2015.01.155.
- [14] S. Abbasi, F. Ahmadpoor, M. Imani et al. *Int J Environ Anal Chem.* **100** (2), 25–240 (2019).
- [15] N. Roozban, S. Abbasi and M. Ghazizadeh, *J Mater Sci* **28** (10), 7343 (2017). doi:10.1007/s10854-017-6421-9.
- [16] P. Gao and D.D. Sun, *Appl. Catal.B-Environ* **147**, 888 (2014). doi:10.1016/j.apcatb.2013.10.025.
- [17] N. Roozban, S. Abbasi and M. Ghazizadeh, *J Mater Sci* **28** (8), 6047 (2017). doi:10.1007/s10854-016-6280-9.
- [18] S. Abbasi, S. Mojtaba Zebarjad, S.H. Noie Baghban et al. *Synthesis and Reactivity in Inorganic, Metal-Organic, and Nano-Metal Chemistry* **45**, 1539 (2015).
- [19] S. Abbasi, S. Mojtaba Zebarjad, S. Hossein Noie Baghban et al., *J Therm Anal Calorim* **123**, 81 (2016). doi:10.1007/s10973-015-4878-4.
- [20] S. Abbasi, M.-S. Ekrami-Kakhki and M. Tahari, *Prog Ind Ecol.* **13** (1), 3 (2019). Xuejing WANG, Shuwen YAO, and Xiaobo LI, *Chinese Journal of Chemistry* **27**, 1317 (2009); K. Byrappa, A. S. Dayananda, C. P. Sajan et al., *journal of materials Science* **43**, 2348 (2008). doi:10.1504/PIE.2019.098760.
- [21] S. Abbasi, S. Mojtaba Zebarjad, S. Hossein Noie Baghban et al., *Bull. Mater. Sci.* **37**(6), 1439 (2014). doi:10.1007/s12034-014-0094-2.
- [22] S. Abbasi, *Mater. Res. Express* **5**, 066302 (2018). doi:10.1088/2053-1591/aac7f4.
- [23] S. Abbasi, S.M. Zebarjad and S. Hossein Noie Baghban, *Engineering* **5**, 207 (2013). doi:10.4236/eng.2013.52030.
- [24] A. Ghaderi, S. Abbasi and F. Farahbod, *Iran. J. Chem. Chem. Eng* **12** (3), 96 (2015).
- [25] A. Hossein Navidpour, M. Fakhrzad, M. Tahari et al., *Surface Eng* **35**(3), 216 (2019). doi:10.1080/02670844.2018.1477559.
- [26] P. Thirukumar, R. Atchudan, A. Shakila Parveen et al., *Sci Rep* **9**(1), 19509 (2019). doi:10.1038/s41598-019-56109-3.
- [27] M. Fakhrzad, A.H. Navidpour, M. Tahari et al., *Mater. Res. Express* **6**(9), 095037 (2019). doi:10.1088/2053-1591/ab2eb5.
- [28] G. Zhu, H. Wang, G. Yang et al., *RSC Adv* **5**(89), 72476 (2015). doi:10.1039/C5RA11873E.